MHD Flow and Heat Transfer of a Dusty Nanofluid over a Stretching Surface in a Porous Medium

Sandeep, N. [1] ***and Saleem, S.*** [2]

[1] Professor, VIT University, India. E-Mail: sandeep@vit.ac.in
[2] 2COMSATS Institute of Information Technology; Pakistan. E-Mail: salmansaleem_33@hotmail.com

ABSTRACT

With every passing day, heat transfer enhancement in convectional base fluids plays a major role in several industrial and engineering processes. During this process, nanofluids attained great importance to enhance the heat transfer rate in convectional flows. Keeping this into view, in this study, we analyzed the MHD flow and heat transfer characteristics of a dusty nanofluid over a stretching surface in the presence of a volume fraction of dust and nano-particles. We have considered two types of nanofluids; namely, CuO-water and Al_2O_3-water immersed with dust particles. The governing partial differential equations are transformed into a set of non-linear ordinary differential equations by using similarity transformation, which are then solved numerically using Runge-Kutta based shooting technique. We found an excellent agreement of the present results with the existing literature. The effects of non-dimensional governing parameters; namely, magnetic field, volume fraction of dust particles, volume fraction of nano-particles, porosity, mass concentration of dust particles and fluid particle interaction on velocity and temperature profiles for both fluid and dust phases are discussed and presented through graphs. Also, skin friction coefficient and local Nusselt number are discussed and presented in tabular form.

KEYWORDS: MHD, Dusty fluid, Nanofluid, Stretching sheet, Volume fraction, Convection, Porous medium.

INTRODUCTION

The momentum and heat transfer characteristics of an MHD flow over a stretching surface have tremendous applications in engineering and applied sciences. Many researchers have investigated the momentum and heat transfer characteristics of either dusty or nanofluids through different channels. In the present study, we are taking initiation to analyze the momentum and heat transfer characteristics of a dusty nanofluid (nanofluid embedded with dust particles) over a stretching surface, by considering volume fraction of dust particles (in μm) and volume fraction of nano-particles (in μm). During the past decade, research on nanofluids was very much developed due to its applications in engineering, such as transportation, micro-mechanics, optical devices, electronics and cooling devices. All these applications are due to the enhancement in heat transfer performance in nanofluids.

Laminar flow of dusty gases was first discussed by Saffman (1962). Hamilton and Crosser (1962) proposed a formulation for the effective thermal conductivity for two-component systems. The behavior of dusty gases at different environments was first analyzed by Marble (1970). Chakrabarti and Gupta (1979) studied MHD flow and heat transfer characteristics over a stretching surface. Bujurke et al. (1987) illustrated heat transfer characteristics of a

Received on 11/9/2015.
Accepted for Publication on 29/11/2016.

second order fluid over a stretching surface. Debnath and Ghosh (1988) discussed an unsteady MHD flow of a dusty fluid between two oscillating plates. Chen and Char (1998) analyzed the heat transfer characteristics of a nanofluid over a continuous stretching surface by considering suction/injection effects. Sattar and Alam (1994) studied MHD heat and mass transfer flow over an accelerated vertical porous plate. Choi (1995) was the first person who introduced the concept of nanofluid. He immersed nanometer-sized particles into a base fluid and observed the increase in heat transfer rate of nano-particle mixed base fluid. Sandeep and Sulochana (2015) analyzed the heat transfer characteristics of a nanofluid by immersing the conducting dust particles. Chen (1998) studied the laminar mixed convection flow over a continuously stretching surface. An unsteady MHD flow over a non-isothermal stretching sheet in a porous medium was studied by Chamkha (1998).

MHD dusty viscoelastic Maxwell fluid flow over a rectangular channel was discussed by Ghosh (2000). Begewadi and Shantharajappa (2000) have considered Frenet Frame and discussed dusty gas flow over it. Stagnation-point flow and heat transfer behavior of Cu-water nanofluid with two different channels were discussed by Sulochana and Sandeep (2015). A mathematical model for dusty gas flow over a naturally occurred porous media was presented by Allan et al. (2004). Elena and Dileep Singh (2009) studied the influence of particle shape on alumina nanofluid flows. Saidu et al. (2010) discussed the convective flow and heat transfer of dusty fluid by considering volume fraction of dust particles. Khan and Pop (2010) studied the boundary layer theories of a nanofluid over a stretching surface. Effect of radiation and viscous dissipation on stagnation-point flow of a micropolar fluid over a nonlinearly stretching surface with suction or injection effects was studied by Jayachandra Babu et al. (2015). Abu-Nada and Chamka (2010) analyzed the natural convection flow of a nanofluid filled with CuO-EG-water with variable thermal properties. Magneto hydrodynamic flow and heat transfer characteristics of a dusty fluid over a stretching surface were presented by Gireesha et al. (2012).

Remeli et al. (2012) considered a Marangoni-driven boundary layer model and discussed the flow and heat transfer characteristics of a nanofluid with suction and injection effects. Dusty viscous fluid flow in a porous medium over a moving hot vertical surface with diffusion effect was analyzed by Anurag Dubey and Singh (2012). Sandeep et al. (2013) analyzed the radiation effects on ethylene glycol-based nanofluids over an infinite vertical plate. Mohan Krishna et al. (2014) analyzed the radiation effect on an unsteady natural convective flow of an MHD nanofluid over a vertical plate by considering heat source effect. Recently, Ramana Reddy et al. (2014) discussed the effects of an aligned magnetic field and radiation on dusty viscous flow by considering heat generation/absorption. Ferdows et al. (2014) have studied the boundary layer flow and heat transfer of a nanofluid over a permeable stretching surface. Dessie et al. (2014) discussed the scaling group analysis on MHD free convective heat and mass transfer over a stretching surface with suction/injection effects.

All the above mentioned studies focused on either dusty or nanofluid flows through different channels. To the authors' knowledge, the present study is a new initiative and no studies have so far been reported on the MHD flow and heat transfer characteristics of a dusty nanofluid over a stretching surface in the presence of a volume fraction of dust and nano-particles in a porous medium. Numerical results have been extracted for this study. The effects of non-dimensional governing parameters on velocity and temperature profiles for both fluid and dust phases are discussed and presented through graphs. Also, skin friction coefficient and Nusselt number are discussed and presented in tabular form.

FLOW ANALYSIS

Consider a steady, two-dimensional, laminar, incompressible and electrically conducting boundary

layer flow of a dusty nanofluid past a stretching sheet. The sheet is along the plane $y=0$ and the flow is being confined to $y>0$. The flow is generated by the two equal and opposite forces acting along the x- axis and the y- axis is normal to it. The sheet is being stretched with the velocity $u_w(x)$ along the x- axis. The flow field is exposed to the influence of the external magnetic field strength B_0 along the x-axis. The dust particles are assumed uniform in size. Spherical shaped nano and dust particles are considered. Number density of dust particles along with volume fraction of dust and nano-particles are taken into account. The boundary layer equations that govern the present flow as per the above assumptions are given as follows:

$$\frac{\partial u}{\partial x}+\frac{\partial v}{\partial y}=0, \tag{1}$$

$$\rho_{nf}(1-\phi_d)\left(u\frac{\partial u}{\partial x}+v\frac{\partial u}{\partial y}\right)=(1-\phi_d)\mu_{nf}\frac{\partial^2 u}{\partial y^2}+KN(u_p-u)-\sigma {B_0}^2 u-\frac{\mu_f}{k_1}u, \tag{2}$$

$$u_p\frac{\partial u_p}{\partial x}+v_p\frac{\partial u_p}{\partial y}=\frac{K}{m}(u-u_p), \tag{3}$$

$$\frac{\partial u_p}{\partial x}+\frac{\partial v_p}{\partial y}=0, \tag{4}$$

with the boundary conditions:

$$\begin{aligned} &u=u_w(x), v=0 \text{ at } y=0,\\ &u\to 0, u_p\to 0, v_p\to v \text{ as } y\to\infty, \end{aligned} \tag{5}$$

where (u,v) and (u_p,v_p) are the velocity components of the nanofluid and dust phases in the x and y directions, respectively, ϕ_d is the volume fraction of dust particles (i. e. , the volume occupied by the dust particles per unit volume of the mixture), μ_{nf} is the dynamic viscosity of the nanofluid, K is the Stokes resistance, m is the mass of the dust particles, N is the number density of dust particles, ρ_{nf} is the density of the nanofluid, σ, B_0 are the electrical conductivity and induced magnetic field, respectively, k_1 is the permeability of the porous medium and $u_w(x)=cx, c>0$ is the stretching sheet velocity. The nanofluid constants are:

$$\begin{aligned} &(\rho c_p)_{nf}=(1-\phi)(\rho c_p)_f+\phi(\rho c_p)_s,\\ &\mu_{nf}=\frac{\mu_f}{(1-\phi)^{2.5}},\\ &\frac{k_{nf}}{k_f}=\frac{(k_s+2k_f)-2\phi(k_f-k_s)}{(k_s+2k_f)+\phi(k_f-k_s)},\\ &\rho_{nf}=(1-\phi)\rho_f+\phi\rho_s, \end{aligned} \tag{6}$$

where ϕ is the volume fraction of nano-particles. The subscripts f and s refer to fluid and solid properties, respectively.

For similarity solution, we introduced the following similarity transformation:

$$\begin{aligned} &u=cxf'(\eta),\ v=-{\nu_f}^{1/2}c^{1/2}f(\eta),\ \eta={\nu_f}^{-1/2}c^{1/2}y,\\ &u_p=cxF'(\eta),\ v_p=-{\nu_f}^{1/2}c^{1/2}F(\eta), \end{aligned} \tag{7}$$

Equation (7) identically satisfies equations (1) and (4). Now, equations (2) and (3) become:

$$\frac{1-\phi_d}{(1-\phi)^{2.5}}f'''-(1-\phi_d)\left(1-\phi+\phi\left(\frac{\rho_s}{\rho_f}\right)\right)(f'^2-ff'')+\alpha\beta(F'-f')-(M+K_1)f'=0, \tag{8}$$

$$F'^2 - FF'' + \beta(F' - f') = 0, \quad (9)$$

with the transformed boundary conditions:

$$f'(\eta) = 1, f(\eta) = 0 \text{ at } \eta = 0,$$
$$f'(\eta) = 0, F'(\eta) = 0, F(\eta) = f(\eta) \text{ as } \eta \to \infty, \quad (10)$$

where $\alpha = Nm/\rho_f$ is the mass concentration of dust particles, $\beta = K/cm$ is the fluid particle interaction parameter for the velocity, $M = \sigma B_0^2/c\rho_f$ is the magnetic field parameter and $K_1 = \nu_f/ck_1$ is the porosity parameter.

HEAT TRANSFER ANALYSIS

The governing boundary layer heat transport equations for dusty nanofluid are:

$$(\rho c_p)_{nf}\left(u\frac{\partial T}{\partial x} + v\frac{\partial T}{\partial y}\right) = k_{nf}\frac{\partial^2 T}{\partial y^2} + \frac{N_1(c_p)_f}{\tau_T}(T_p - T) + \frac{N_1}{\tau_v}(u_p - u)^2, \quad (11)$$

$$N_1 c_m\left(u_p\frac{\partial T_p}{\partial x} + v_p\frac{\partial T_p}{\partial y}\right) = -\frac{N_1(c_p)_f}{\tau_T}(T_p - T), \quad (12)$$

where T and T_p are the temperature of nanofluid and dust particles, respectively, k_{nf} is the effective thermal conductivity of the nanofluid, $(c_p)_f, c_m$ are the specific heat of the fluid and dust particles, respectively, $N_1 = Nm$ is the density of the particle phase, τ_T is the thermal equilibrium time and τ_v is the relaxation time of dust particles.

We considered temperature boundary conditions in order to solve equations (11) and (12) as:

$$T = T_w = T_\infty + A(x/l)^2 \text{ at } y = 0,$$
$$T \to T_\infty, T_p \to T_\infty \text{ as } y \to \infty, \quad (13)$$

where T_w, T_∞ are the temperatures near the wall and far away from the wall, respectively and $l = \nu_f^{1/2} c^{-1/2} > 0$ is a characteristic length.

We now introduce the following non-dimensional variables to get the similarity solutions of equations (11) and (12).

$$\theta(\eta) = \frac{T - T_\infty}{T_w - T_\infty}, \theta_p(\eta) = \frac{T_p - T_\infty}{T_w - T_\infty}, \quad (14)$$

where $T - T_\infty = A(x/l)^2\theta(\eta), A > 0$.

Using Eqs. (13) and (14) in Eqs. (11) and (12), we get the ordinary differential equations as:

$$\frac{1}{Pr}\frac{k_{rf}/k_f}{1-\emptyset+\emptyset\,((pc_p)_s/(pc_p)_f)}\theta'' - (2f'\theta - f\theta') + \frac{1}{1-\emptyset+\emptyset\,((pc_p)_s/(pc_p)_f)}\left[\alpha\,\beta_T\,(\theta_p - \theta) + Ecos\,(F' - f')^2\right] = 0, \quad (15)$$

$$2F'\theta_p - F\theta_p' + \gamma\beta_T(\theta_p - \theta) = 0, \quad (16)$$

where $\Pr = \nu_f/\alpha_f$ is the Prandtl number, $\beta_T = 1/c\tau_T$ is the fluid particle interaction parameter for temperature, $Ec = cl^2/\mathrm{A}(c_p)_f$ is the Eckert number, $\gamma = (c_p)_f/c_m$ is the ratio of specific heat of the fluid to that of the dust particles.

The transformed boundary conditions are:

$$\theta(\eta) = 1 \text{ at } \eta = 0,$$
$$\theta(\eta) = 0, \theta_p(\eta) = 0 \quad \text{as } \eta \to \infty, \quad (17)$$

For the engineering interest, the skin friction coefficient C_f and the local Nusselt number Nu_x are defined as:

$$C_f = \tau_w / \rho_{nf} u_w^2, Nu_x = x q_w / k_{nf}(T_w - T_\infty), \quad (18)$$

where the surface shear stress τ_w and the surface heat flux q_w are given by:

$$\tau_w = \mu_{nf}\left(\frac{\partial u}{\partial y}\right)_{y=0}, \; q_w = -k_{nf}\left(\frac{\partial T}{\partial y}\right)_{y=0}, \quad (19)$$

Using non-dimensional variables, we get:

$$C_f \, \mathrm{Re}_x^{1/2} = f''(0), \mathrm{Nu}_x \, \mathrm{Re}_x^{-1/2} = -\theta'(0), \quad (20)$$

where $Re_x = u_w x / v_{nf}$ is the local Reynolds number.

RESULTS AND DISCUSSION

The coupled ordinary differential equations (8), (9), (15) and (16) subject to the boundary conditions as in equations (10) and (17) are solved numerically using Runge-Kutta based shooting technique. The results obtained show the influences of the non-dimensional governing parameters; namely: magnetic field parameter M ,volume fraction of dust particles ϕ_d, volume fraction of nano-particles ϕ, porosity parameter K , mass concentration of the dust particles α, fluid particle interaction parameter for velocity β and fluid particle interaction parameter for temperature β_T on velocity and temperature profiles for fluid and dust phases for CuO-water and Al_2O_3-water dusty nanofluids. These influences were discussed and presented in tabular form. Also, skin friction coefficient and Nusselt number are discussed and presented through tables. For numerical results, we considered $\beta_T = \alpha = K = 0.2,\ \beta = 0.5, E_c = 3,\ \emptyset = \emptyset_d = 0.1,\ M = 1$. These values were kept constant in the entire study as shown in the figures. The thermo-physical properties of water, copper oxide (CuO) and aluminum oxide (Al_2O_3) are given in Table 1.

Table 1. Thermo-physical properties of base fluid and different nano-particles

	$\rho(Kg\,m^{-3})$	$c_p(J\,Kg^{-1}\,K^{-1})$	$k(Wm^{-1}\,K^{-1})$
H_2O	997. 1	4179	0. 613
CuO	6320	531. 8	76. 5
Al_2O_3	3970	765	40

Figs. 1 and 2 depict the variation in velocity and temperature profiles for fluid and dust phases for different values of the magnetic field parameter (M). It is evident that an increase in the magnetic field parameter depreciates the velocity profiles and enhances the temperature profiles of both fluid and dust phases. Generally, an increase in the magnetic field develops the opposite force to the flow, which is called Lorentz force. This force declines the velocity boundary layer and improves the thermal boundary layer. We noticed an interesting result; namely that an increase in the magnetic field parameter improves the temperature profiles of CuO-water dusty nanofluid compared with those of Al_2O_3-water dusty nanofluid. Figs. 3 and 4 illustrate the variation in velocity and temperature profiles for fluid and dust phases of CuO-water and Al_2O_3-water dusty nanofluids for different values of volume fraction of nano-particles (ϕ). It is clear from Figure 3 that an increase in the volume fraction of nano-particles enhances the velocity profiles of the fluid and dust phases. But from Figure 4, we observe an arousing result; namely that an increase in the volume fraction of nano-particles increases the temperature profiles of the fluid phase, but declines the

temperature profiles of the dust phase. We may explain this phenomenon by that increased values of volume fraction of the nano-particles enhance the thermal conductivity of the fluid due to good interaction with the base fluid. But, in dust phase, the mean interacting time between particles is longer than that between fluid and particles.

Figs. 5 and 6 show the variation in velocity and temperature profiles for fluid and dust phases of CuO-water and Al_2O_3-water dusty nanofluids for different values of volume fraction of dust particles (ϕ_d). It is clear that an enhancement in the volume fraction of dust particles depreciates the velocity profiles and improves the temperature profiles of both fluid and dust phases. Generally, size of dust particles is in micro/millimeters. So, an increase in the volume fraction of dust particles enhances the volume occupied by dust particles. These particles slow down the velocity profiles due to shear stress near the walls. We have noticed a slight enhancement in the temperature profiles of both fluid and dust phases due to increased thermal conductivity. Here, it is worth mentioning that from Figs. 4 and 6, it is found that the increasing sense in the temperature profiles is due to an increase in the volume fraction of nano-particles. But, we have seen a very small amount of increment in the temperature profiles with an increase in the volume fraction of dust particles. This proves that nano-particles are effective thermal enhancement materials while compared with dust particles. Figs. 7 and 8 display the variation in velocity and temperature profiles for fluid and dust phases for different values of porosity parameter (K). It is evident from these figures that an increase in the porosity parameter decreases the velocity profiles and increases the temperature profiles of both fluid and particle phases. This is due to the fact that increasing values of porosity parameter widen the porous layers, thereby leading to decline the velocity profiles. But, porosity parameter has a tendency to generate internal heat to the flow, thereby improving the temperature profiles of both fluid and dust phases.

Figs. 9 and 10 reveal the variation in velocity and temperature profiles for fluid and dust phases for different values of mass concentration of dust particles (α). It is observed that an increase in the mass concentration of dust particles depreciates the velocity profiles of the fluid and dust phases and boosts the temperature profiles for both phases. Generally, an increase in mass concentration of dust particles means an increase in the number density of dust particles. It is expected that if the number density of dust particles increases, then this declines the velocity profiles and enhances the thermal boundary layer thickness. This agrees with the general fact. Figs. 11 and 12 depict the variation in velocity and temperature profiles for fluid and dust phases for different values of fluid particle interaction parameter for velocity (β). It is noticed that an increase in the fluid particle interaction parameter increases the velocity and temperature profiles of the dust phase and decreases the velocity and temperature profiles of the fluid phase for both fluids. This is due to the fact that the interaction between fluid and particles is high, causing the particle phase to slow down the fluid velocity till particle velocity reaches fluid velocity. During this time interval, the particle phase continuously dominates the fluid phase till both are having equal velocities. The enhancement in temperature profiles is due to improvement in thermal conductivity. Fig. 13 shows the variation in temperature profiles for fluid and dust phases for different values of fluid particle interaction parameter for temperature (β_T). It is clear that an increase in the fluid particle interaction parameter for temperature depreciates the temperature profiles for both fluid and dust phases. A uniform depreciation in temperature profiles of both dusty nanofluids is noticed with an increment in β_T. Physically, increasing the values of β_T develops the opposite force to the flow and reduces the thermal boundary layer thickness.

Tables 2 and 3, respectively, represent the effects of various non-dimensional governing parameters on skin friction coefficient and Nusselt number forAl_2O_3-water and CuO-water dusty nanofluids. It is observed from the tables that enhancing the values of magnetic field parameter, volume fraction of nano-particles, volume

fraction of dust particles, porosity parameter and mass concentration of dust particles depreciates friction factor along with heat transfer rate in both dusty nanofluids. But, an increase in the volume fraction of dust particles causes a partial decrement in heat transfer rate. Increasing fluid particle interaction parameters for velocity and temperature causes an enhancement in heat transfer rate in both dusty nanofluids. But, we have seen negligible depreciation in friction factor of Al_2O_3-water dusty nanofluid by an increase in fluid particle interaction parameter for temperature. Increasing the value of fluid particle interaction parameter for velocity does not show any effect on friction factor of CuO-water dusty nanofluid.

Table 4 shows the validation of the present results with the existing results of Gireesha et al. (2012) under some special assumptions. We found an excellent agreement of the present results with the existing results. This proves the validity of the present study along with the numerical technique used in this study.

Table 2. Variation in $f''(0)$ and $-\theta'(0)$ for Al_2O_3-water dusty nanofluid

M	ϕ	ϕ_d	K	α	β	β_T	$f''(0)$	$-\theta'(0)$
1							-1. 457159	0. 903659
2							-1. 718783	0. 880113
3							-1. 948723	0. 860485
	0. 1						-1. 457159	0. 903659
	0. 2						-1. 333432	0. 817393
	0. 3						-1. 196284	0. 750765
		0. 1					-1. 457159	0. 903659
		0. 2					-1. 501215	0. 899615
		0. 3					-1. 556302	0. 894596
			0				-1. 399948	0. 908937
			1				-1. 669340	0. 884475
			2				-1. 904806	0. 864145
				1			-1. 531881	0. 761492
				2			-1. 620737	0. 601848
				3			-1. 705198	0. 458506
					0. 1		-1. 443125	0. 874154
					0. 2		-1. 447503	0. 884351
					0. 3		-1. 451218	0. 892317
						0. 5	-1. 457162	0. 911415
						1. 0	-1. 457162	0. 928952
						1. 5	-1. 457159	0. 948222

Table 3. Variation in $f''(0)$ and $-\theta'(0)$ for CuO-water dusty nanofluid

M	ϕ	ϕ_d	K	α	β	β_T	$f''(0)$	$-\theta'(0)$
1							-1. 516978	0. 899035
2							-1. 770328	0. 876493
3							-1. 994516	0. 857584
	0. 1						-1. 516978	0. 899035
	0. 2						-1. 428711	0. 811899
	0. 3						-1. 307909	0. 746173
		0. 1					-1. 516978	0. 899035
		0. 2					-1. 559488	0. 895173
		0. 3					-1. 612731	0. 890377
			0				-1. 461883	0. 904041
			1				-1. 722293	0. 880680
			2				-1. 951605	0. 861118
				1			-1. 589037	0. 761923
				2			-1. 674992	0. 607177
				3			-1. 756941	0. 467576
					0. 1		-1. 503485	0. 870542
					0. 2		-1. 507696	0. 880409
					0. 3		-1. 511269	0. 888098
						0. 5	-1. 516987	0. 906827
						1. 0	-1. 516987	0. 924408
						1. 5	-1. 516987	0. 943656

Table 4. Comparison of the present results with existing studies in the presence of Prandtl number

Pr	Gireesha et al. (2015)	Present Study
0. 72	1. 0886	1. 088561
1	1. 3333	1. 333333
10	4. 7968	4. 796817

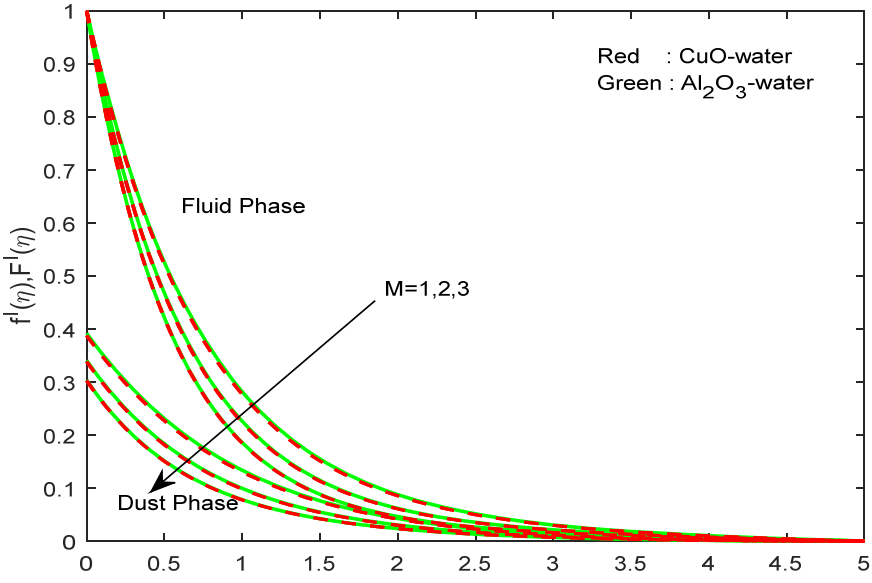

Figure (1): Velocity profiles of fluid and dust phases for various values of M

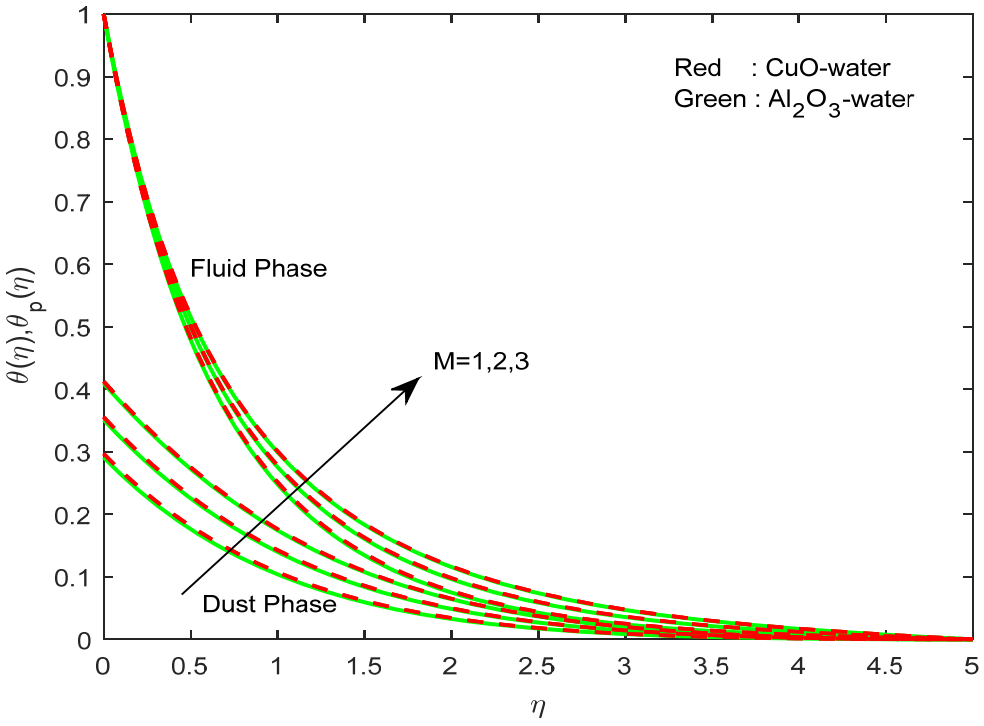

Figure (2): Temperature profiles of fluid and dust phases for various values of M

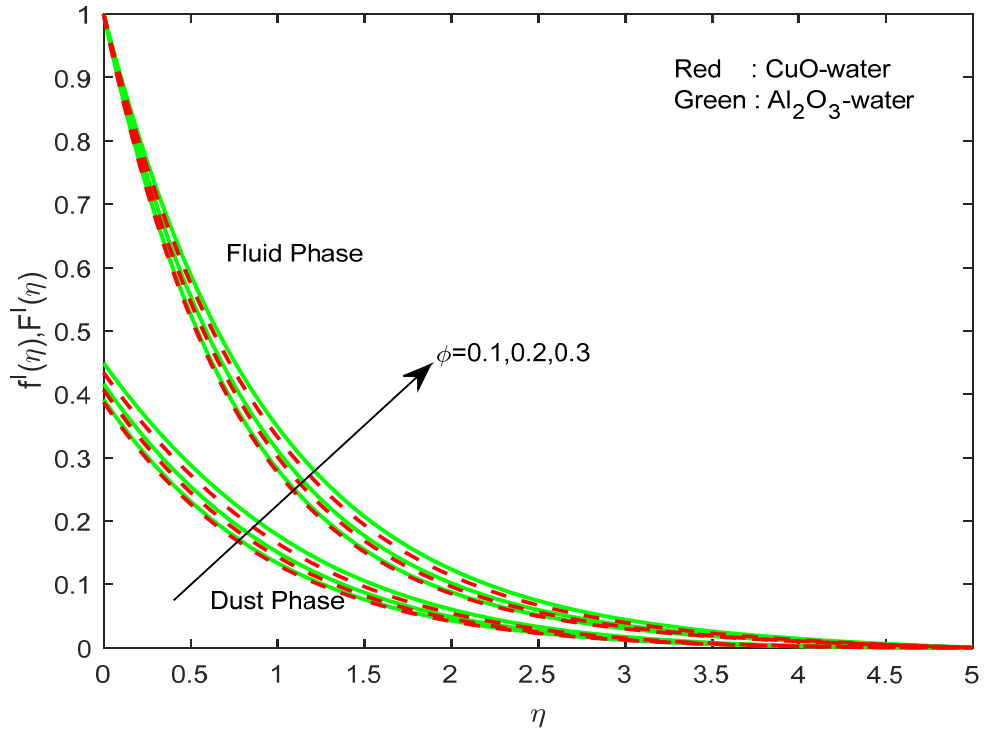

Figure (3): Velocity profiles of fluid and dust phases for various values of ϕ

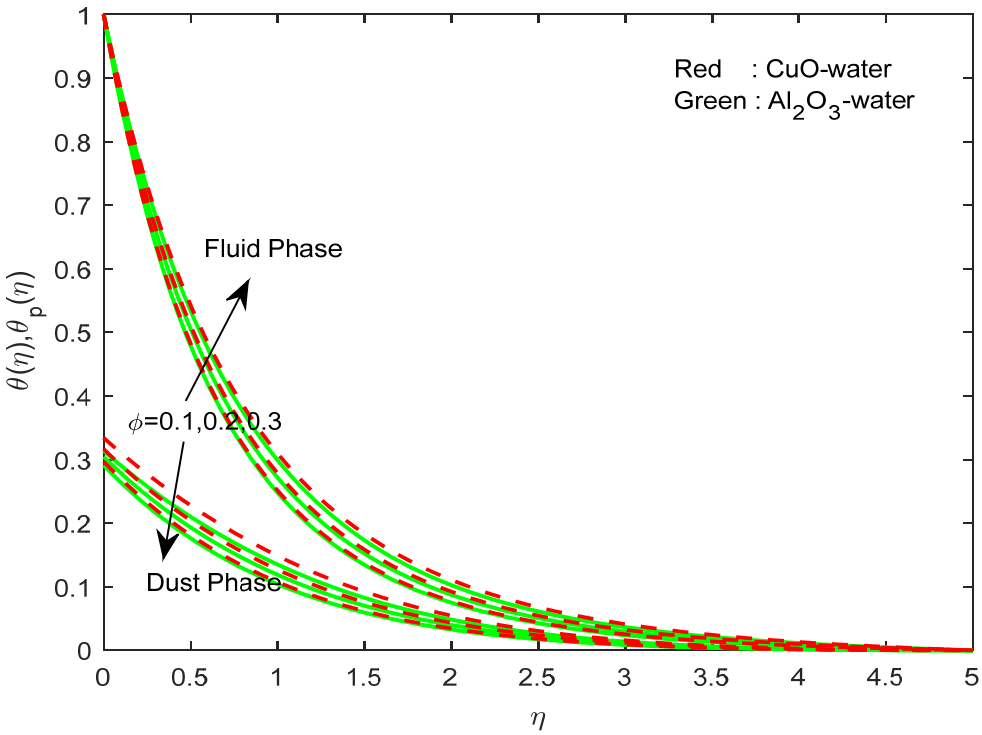

Figure (4): Temperature profiles of fluid and dust phases for various values of ϕ

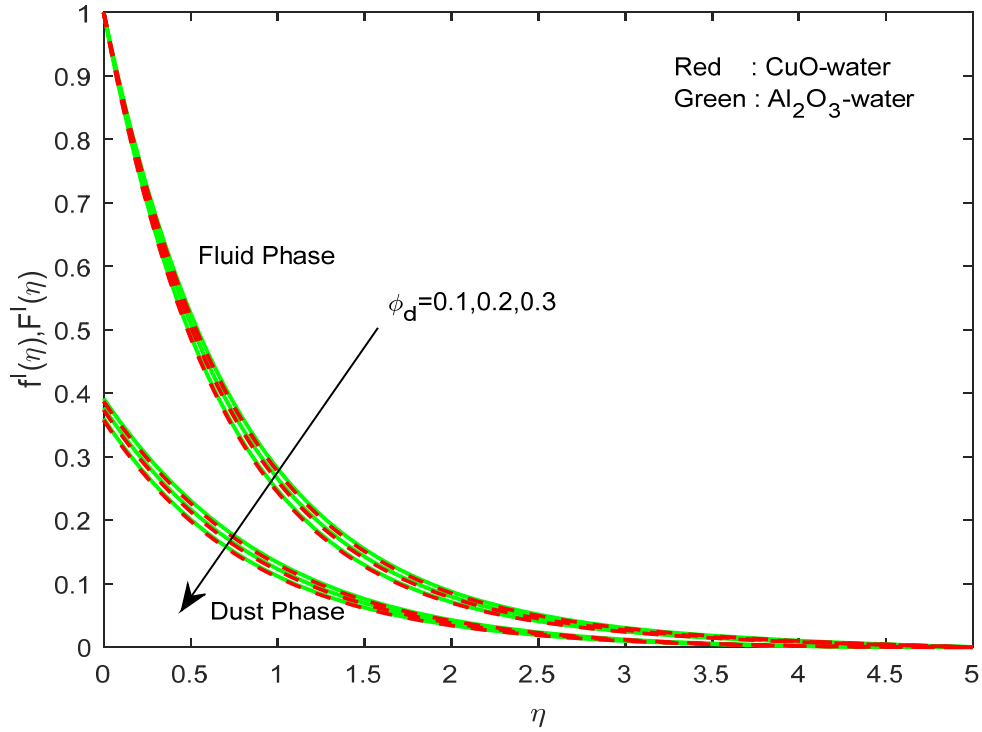

Figure (5): Velocity profiles of fluid and dust phases for various values of ϕ_d

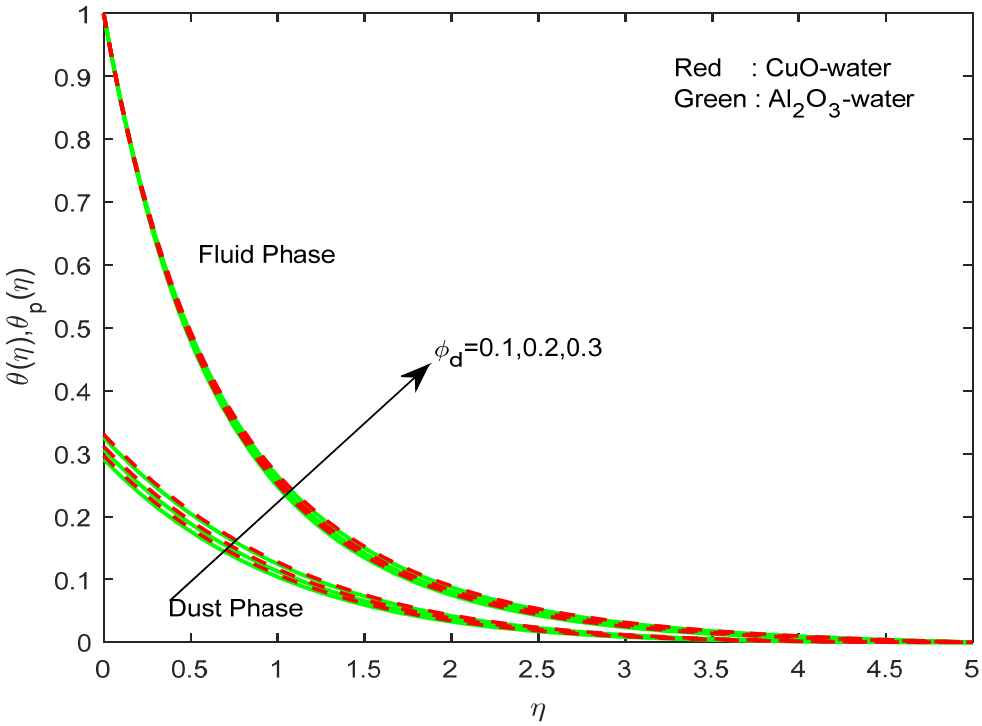

Figure (6): Temperature profiles of fluid and dust phases for various values of ϕ_d

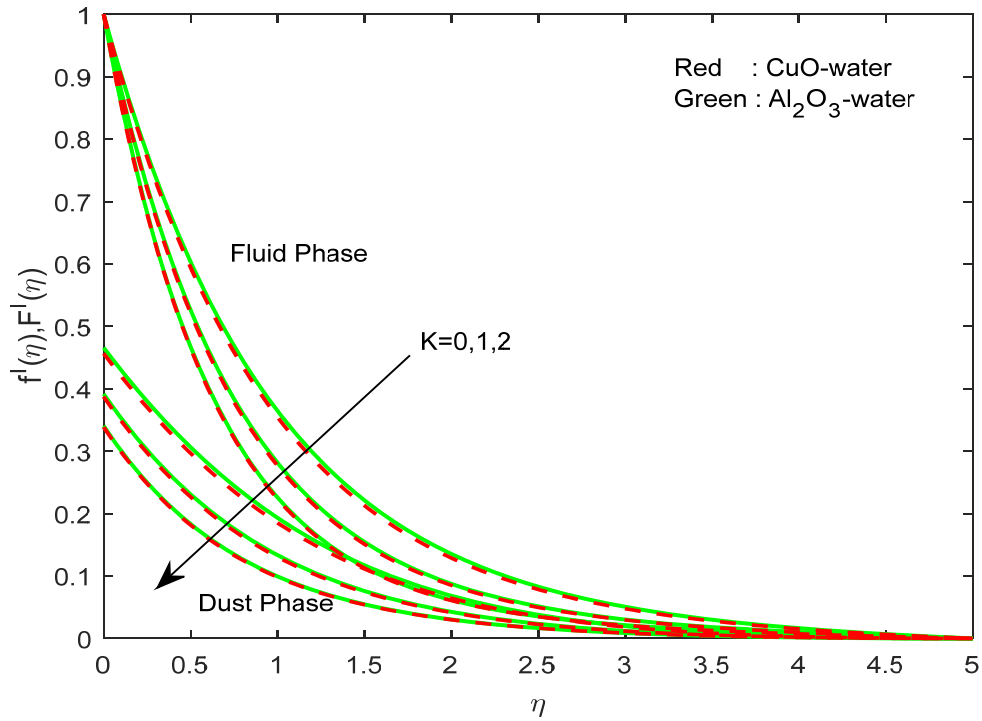

Figure (7): Velocity profiles of fluid and dust phases for various values of *K*

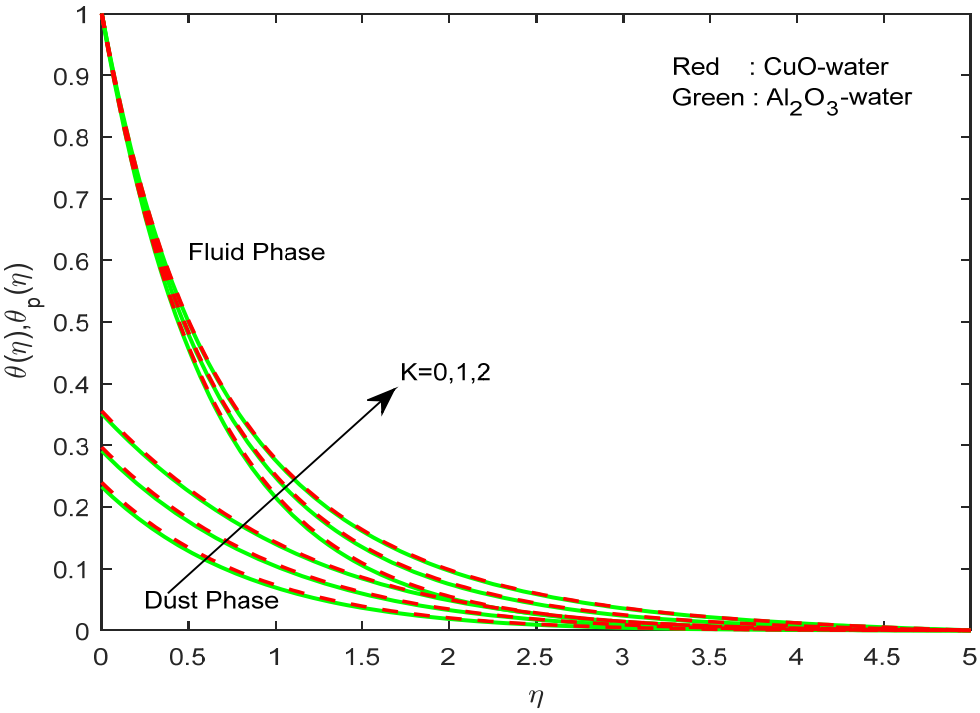

Figure (8): Temperature profiles of fluid and dust phases for various values of *K*

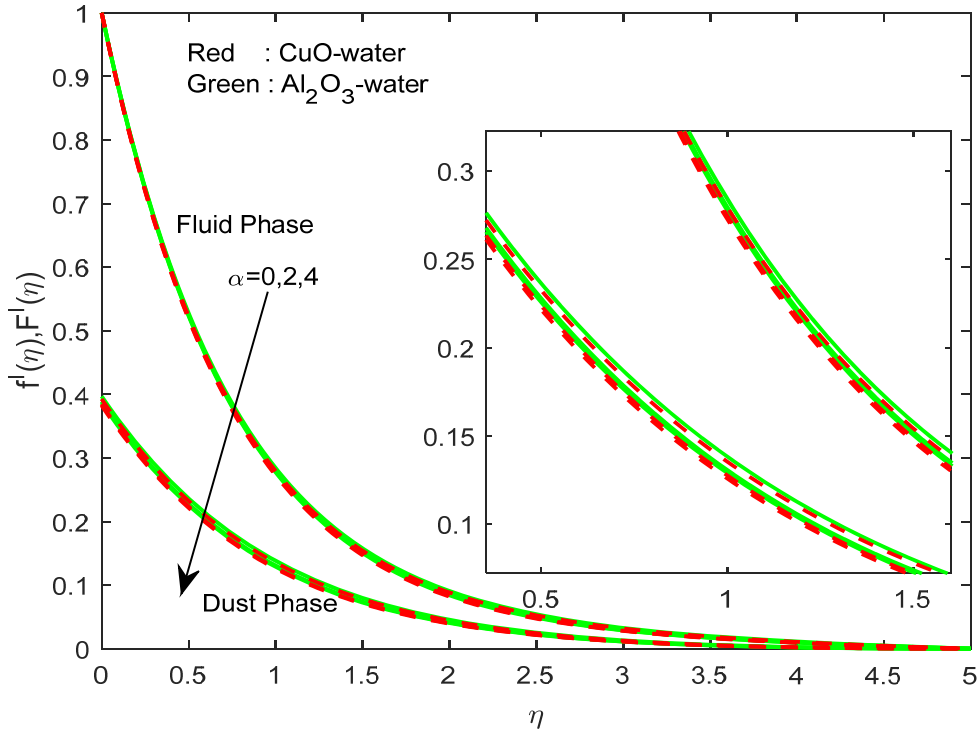

Figure (9): Velocity profiles of fluid and dust phases for various values of α

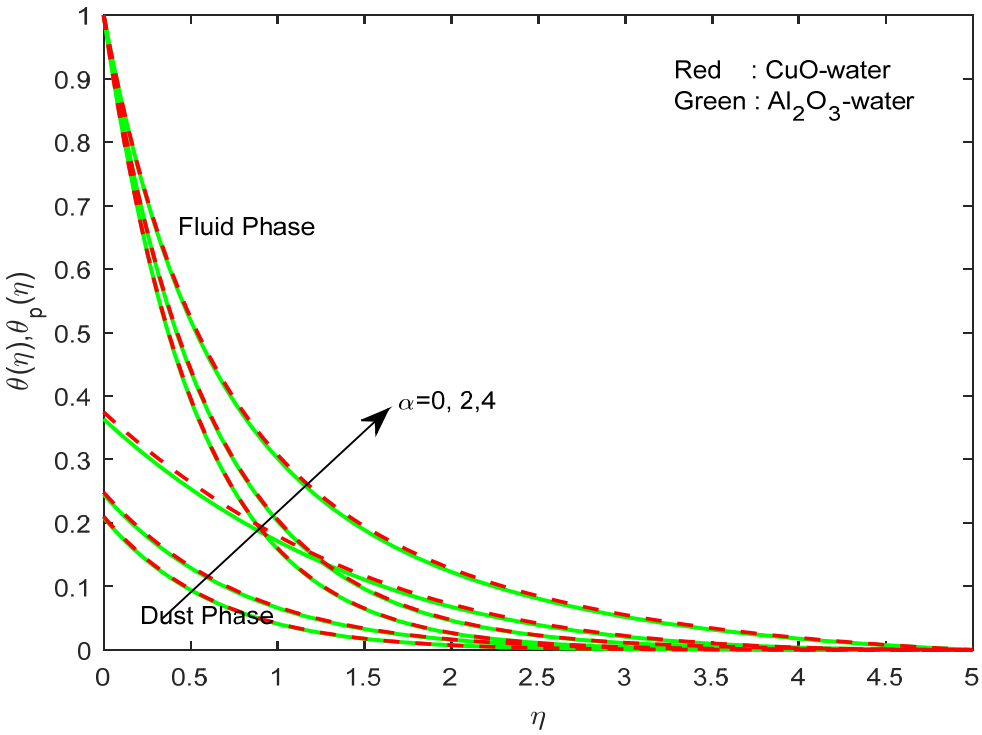

Figure (10): Temperature profiles of fluid and dust phases for various values of α

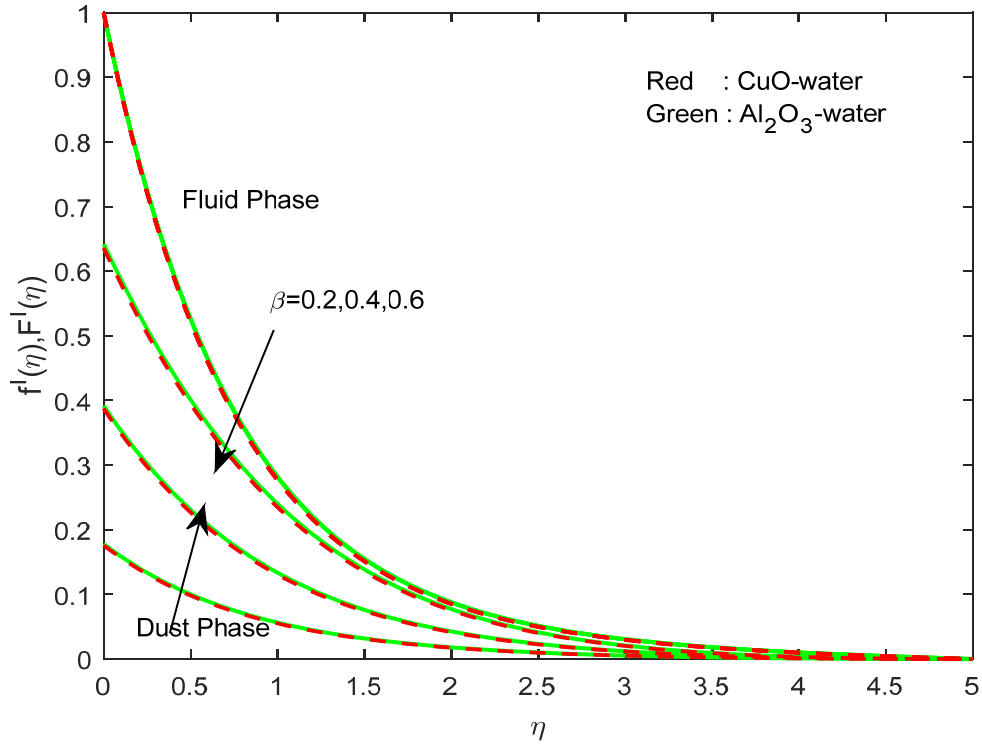

Figure (11): Velocity profiles of fluid and dust phases for various values of β

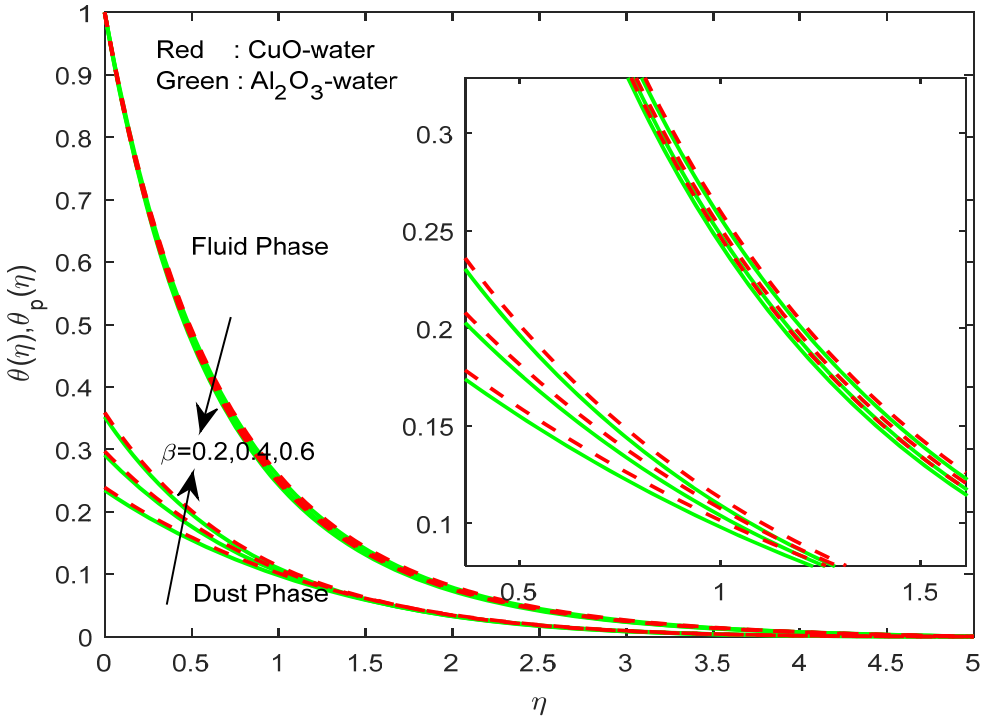

Figure (12): Temperature profiles of fluid and dust phases for various values of β

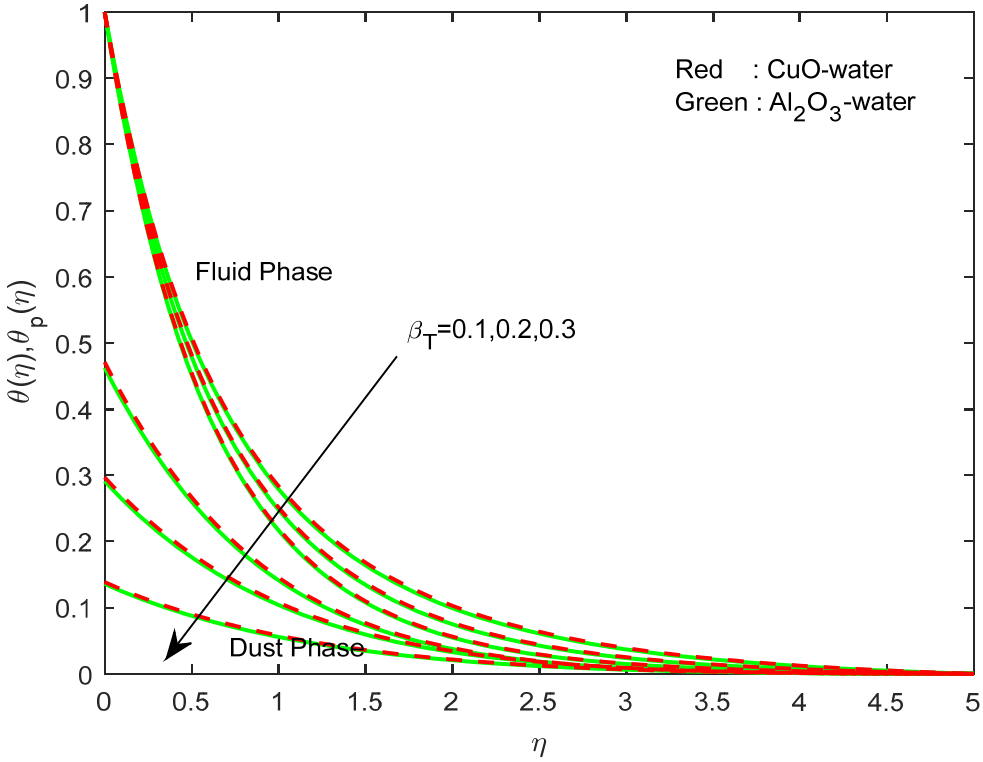

Figure (13): Temperature profiles of fluid and dust phases for various values of β_T

CONCLUSIONS

In this study, we presented the numerical results for analyzing the momentum and heat transfer characteristics of MHD flow of a dusty nanofluid over a stretching surface in the presence of volume fraction of dust and nano-particles in a porous medium. We considered CuO-water and Al_2O_3-water nanofluids immersed with dust particles. The effects of non-dimensional governing parameters on velocity and temperature profiles for both fluid and dust phases are discussed and presented through graphs. Also, skin friction coefficient and Nusselt number are discussed and presented for two dusty nanofluids separately in tabular form.

The conclusions of the present study are as follows:

- An increase in fluid particle interaction enhances the heat transfer rate.
- An increase in the volume fraction of dust particles and volume fraction of nano-particles improves the temperature profiles of the flow. This effect is higher on CuO-water dusty nanofluid compared with that on Al_2O_3-water dusty nanofluid.
- Enhancement in mass concentration of dust particles declines the velocity boundary layer thickness and improves the temperature boundary layer thickness.
- A rise in the value of fluid particle interaction parameter for velocity depreciates the velocity profiles of fluid phase, but improves the velocity of dust phase.

REFERENCES

Abu-Nada, E., and Chamkha, A.J. (2010). "Effect of nanofluid variable properties on natural convection in enclosures filled with a CuO-EG-water nanofluid". Int.J. of Thermal Sci. , 49, 2339-2352.

Allan, F.M., Qatanani, N., Barghouthi, I., and Takatka, M.K. (2004). "Dusty gas model of flow through naturally occurring porous media". App. Math.Comp., (148), 809-821.

Anurag Dubey, and Singh, U.R. (2012). "Effect of dusty viscous fluid on unsteady laminar free convective flow through a porous medium along a moving porous hot vertical sheet with thermal diffusion". Applied Mathematical Sciences, 6, 6109-6124.

Begewadi, C.S., and Shantharajappa, A.N. (2000). "A study of unsteady dusty gas flow in Frenet Frame field". Ind. J. Pure and App. Math., 31, 1405-1420.

Bujurke, N.M., Biradar, S.N., and Hiremath, P.S. (1987). "Second-order fluid flow past a stretching sheet with heat transfer". Z. Angew Math.Phys., 38, 653-657.

Chamkha, A. J. (1998). "Unsteady hydro-magnetic flow and heat transfer from a non-isothermal stretching sheet immersed in a porous medium". Int.Comm. in Heat and Mass Transfer, 25, 899-906.

Charkrabarti, A., and Gupta, A.S. (1979). "Hydro-magnetic flow and heat transfer over a stretching sheet". Quart.Appl.Math., 37, 73-78.

Chen, C.H. (1998). "Laminar mixed convection adjacent to vertical, continuously stretching sheets". Heat Mass Transfer, 33, 471-476.

Chen, C.K., and Char, M.I. (1998). "Heat transfer of a continuous stretching surface with suction or blowing". J. Math. Anal. Appl., 135, 568-580.

Choi, S.U.S. (1995). "Enhanced thermal conductivity of nanofluids with nano-particles, development and applications of Newtonian flows". FED, 66, 99-105.

Debnath, L., and Ghosh, A.K. (1988). "On unsteady hydromagnetic flows of a dusty fluid between two oscillating plates. "Appl. Sci. Res., 45, 353-356.

Dessie, H., and Kishan, N. (2014). “Scaling group analysis on MHD free convective heat and mass transfer over a stretching surface with suction/injection, heat source/sink considering viscous dissipation and chemical reaction effects”. Applications and Applied Mathematics: An International Journal, 9 (2), 553-572.

Elena, V.T., and Dileep Singh, J. L. R. (2009). “Particle shape effect on thermo-physical properties of alumina nanofluids”. Journal of Applied Physics, 106, DOI: 10. 1063/1. 3155999.

Ferdows, M.S., Chapal, M., and Afify, A.A. (2014). “Boundary layer flow and heat transfer of a nanofluid over a permeable unsteady stretching sheet with viscous dissipation”. J. Eng. Thermo-physics, 23, 216-228.

Ghosh, B.C. (2000). “Hydromagnetic flow of a dusty viscoelastic Maxwell fluid through a rectangular channel”. Int. J. Appl. Mech. Eng., 7, 591-618.

Gireesha, B.J., Roopa, G.S., Lokesh, H.J., and Bagewadi, C.S. (2012). “MHD flow and heat transfer of a dusty fluid over a stretching sheet”. Int. J. Phys. and Math. Sci., 3, 171-180.

Hamilton, R.L., and Crosser, O.K. (1962). “Thermal conductivity of heterogeneous two-component systems". J. of Industrial and Eng. Chemistry Fundamentals, 1 (3), 187-191.

Jayachandra Babu, M., Radha Gupta, and Sandeep, N. (2015). “Effect of radiation and viscous dissipation on stagnation-point flow of a micropolar fluid over a non-linearly stretching surface with suction/injection". J. of Basic and Applied Research Int., 7, 73-82

Khan, W.A., and Pop, I. (2010). “Boundary-layer flow of a nanofluid past a stretching sheet”. Int. J. Heat Mass Trans., 53, 2477–2483.

Marble, F.E. (1970). “Dynamics of dusty gases”. Annual Review of Fluid Mechanics, 2, 397-446. DOI: 10. 1146/annurev. fl. 02. 010170. 002145.

Mohankrishna, P., Sugunamma, V., and Sandeep, N. (2014). “Radiation and magnetic field effects on unsteady natural convection flow of a nanofluid past an infinite vertical plate with heat source”. Chemical and Process Engineering Research, 25, 39-52.

Ramana Reddy, J.V., Sugunamma, V., Mohan Krishna, P., and Sandeep, N. (2014). “Aligned magnetic field, radiation and chemical reaction effects on unsteady dusty viscous flow with heat generation/absorption”. Chemical and Process Eng. Research, 27, 37-53.

Remeli, A., Arifin, N.M., Ismail, F., and Pop, I. (2012). “Marangoni driven boundary layer flow in a nanofluid with suction/injection”. World Applied Sciences Journal, 17, 21-26.

Saffman, P.G. (1962). "On the stability of laminar flow of a dusty gas". J. Fluid Dynamics, 13, 120-128.

Saidu, I., Waziri, M.M., Abubakar Roko, and Hamisu, M. (2010). “MHD effects on convective flow of dusty viscous fluid with volume fraction of dust particles”. ARPN J. of Eng. and Applied Sciences, 5, 86-91.

Sandeep, N., Sugunamma, V., and Mohan Krishna, P. (2013). “Effects of radiation on an unsteady natural convective flow of an EG-nimonic 80 nanofluid past an infinite vertical plate”. Int. Journal of Advances in Physics Theories and Applications, 23, 36-43.

Sandeep, N., and Sulochana, C. (2015). “MHD flow of a dusty nanofluid over a stretching surface with volume fraction of dust particles”. Ain Shams Engineering Journal (In Press).

Sattar, M.A., and Alam, M.M. (1994). “Thermal diffusion as well as transpiration effects on MHD free convection and mass transfer flow past an accelerated vertical porous plate”. Indian J. Pure App. Math., 25, 679-688.

Sulochana, C., and Sandeep, N. (2015). “Stagnation-point flow and heat transfer behavior of Cu-water nanofluid towards horizontal and exponentially stretching/shrinking cylinders”. Applied Nanoscience, 5, 451-460.